Proceedings of the ASME 2022 17th International Manufacturing Science and Engineering Conference
MSEC2022
June 27- July 1, 2022, Virtual, Online

MSEC2022-85534

PRECISION EVALUATION OF LARGE PAYLOAD SCARA ROBOT FOR PCB ASSEMBLY

Andrew S. Nimon
Louisville Automation & Robotics Research Institute
University of Louisville
Louisville, KY

Andriy Sherehiy
Louisville Automation & Robotics Research Institute
University of Louisville
Louisville, KY

Moath Alqatamin
Louisville Automation & Robotics Research Institute
University of Louisville
Louisville, KY

Danming Wei
Louisville Automation & Robotics Research Institute
University of Louisville
Louisville, KY

Dan O. Popa
Louisville Automation & Robotics Research Institute
University of Louisville
Louisville, KY

ABSTRACT

The placement of SMD components is usually performed with Cartesian type robots, a task known as pick-and-place (P&P). Small Selective Compliance Articulated Robot Arm (SCARA) robots are also growing in popularity for this use because of their quick and accurate performance. This paper describes the use of the Lean Robotic Micromanufacturing (LRM) framework applied on a large, 10kg payload, industrial SCARA robot for PCB assembly. The LRM framework guided the precision evaluation of the PCB assembly process and provided a prediction of the placement precision and yield. We experimentally evaluated the repeatability of the system, as well as the resulting collective errors during the assembly. Results confirm that the P&P task can achieve the required assembly tolerance of 200 microns without employing closed-loop visual servoing, therefore considerably decreasing the system complexity and assembly time.

1. INTRODUCTION

Automated assembly of surface mount technology (SMT) printed circuit boards (PCBs) is typically performed by machines executing discrete tasks such as solder paste application, pick and placement of the surface mount devices (SMDs), inspections, and solder paste reflow [1]. The placement of SMD components is usually performed with Cartesian type robots, a task known as pick-and-place (P&P).

Smaller (<10kg payload) Selective Compliance Articulated Robot Arm (SCARA) robots are growing in popularity for this use because of their lower cost and ability to accurately pick up and place very small SMD components. However, these smaller SCARA robots have limitations regarding payload capacity and workspace reach, which limit their ability to handle additional process tools such as grippers, dispensers, soldering guns, and cameras. Larger robots are typically not used for PCB P&P work because of their mass and the perceived lack of precision.

Precision metrics for robots are formally defined in ISO 9283 which provide standard methods to specify and test performance characteristics of manipulating industrial robots for repeatability, accuracy, and stability [3]. Precision analysis on robots using ISO 9283 have been discussed in a number of papers, [2] [4] [5]. Robot manufacturers are expected to follow this standard and provide listed repeatability for their robots as one of the specifications. However, this standard does not cover changing or uncertain operating conditions for robots such as payloads, calibration sensors, and friction [6]. Additionally, the framework holding the robot and the workpiece will greatly affect the overall performance of a robot. Therefore, it is necessary for the user to be able to perform precision analysis on the robot in the specific location and application to determine the system's accuracy and repeatability.

Although many papers have been written on assessing or improving a robot's repeatability and accuracy [7] [8], few have provided a systematic methodology for determining a robotic manufacturing system's precision and control. This paper describes, implements, and validates one such methodology, the Lean Robotic Micromanufacturing (LRM) [6], applied to robotic PCB assembly process. The LRM framework enables the use of large payload SCARA robots for this task and selects an appropriate controller to achieve the required precision for P&P of electronic components.

LRM provides a design framework with assessment tools, statistical analysis, and a decision matrix. The LRM process includes the determination of a robotic system's accuracy and repeatability, a framework for any necessary system redesign, and a decision matrix for applying an optimal control strategy to meet the design specifications and yield requirements. With the

decision matrix, a precision-adjusted hybrid controller can be employed to switch the control mode between open, closed, and calibrated operation as needed within the assembly chain.

The contribution of this paper is to apply the LRM analysis for the P&P of SMD components with a large 10 kg payload industrial SCARA robot. Our analysis predicts that open-loop control is sufficient during operation of the robot, therefore increasing assembly rate and system flexibility, while reducing system complexity. By using a large payload SCARA robot with a tool changer, all PCB operations and tools can be handled by a single robot, thereby reducing manual intervention, reducing failure rates, and increasing flexibility to handle new PCB designs and requirements.

The paper is organized as follows: in Section 2 we describe the tools and methods used to implement the pick and place assembly, including the robotic equipment, the PCB and SMD components, and a more detailed description of the LRM framework. Section 3 details the experimental procedures used for the precision analysis, and Section 4 covers the experimental results and discussion about results. Finally, Section 5 provides a conclusion of the paper and discusses future work.

2. DESCRIPTION OF TOOLS AND METHODS

2.1 NeXus System

The SCARA robot evaluated in this paper is part of a custom multiscale manufacturing and assembly instrument called NeXus, designed, and built at the University of Louisville. The system combines industrial robots, precision positioners and manipulators, custom fused deposition modeling (FDM) 3D printing, 30-micron (μm) line width aerosol inkjet printing, ultrasonic bonding, intense pulse light sintering, and various metrology, microscopy, and testing instruments, see Figure 1.

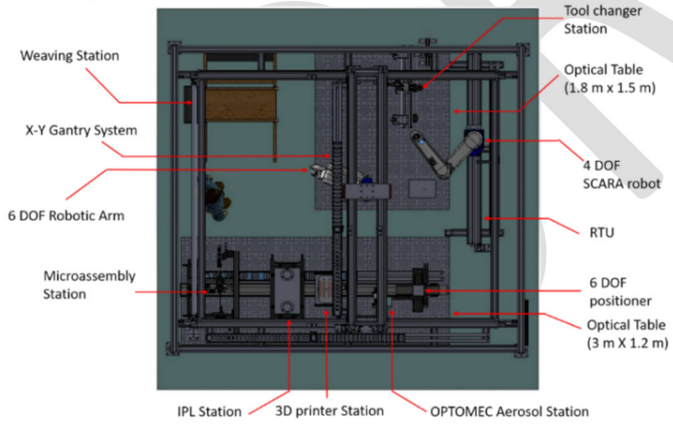

(a)

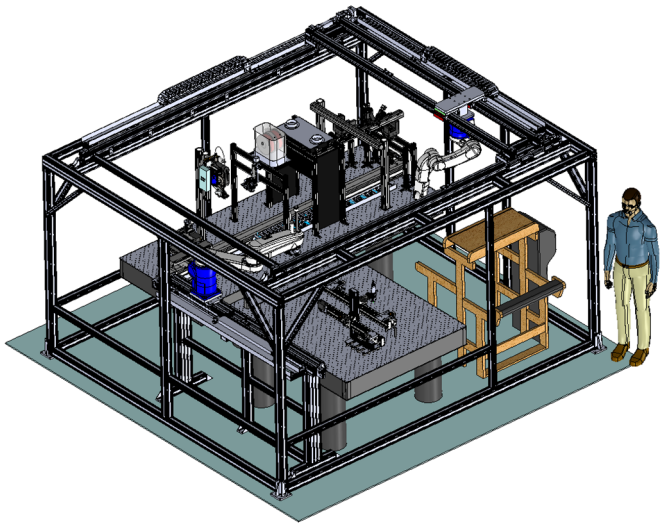

(b)

FIGURE 1: NEXUS SYSTEM TOP VIEW (a) and ISO VIEW (b)

The NeXus system includes two industrial robotic arms. One is a six-degree-of-freedom (6DOF) robot, inverted on an X-Y gantry (DENSO VS-6577-B). The other is a 4DOF Selective Compliance Articulated Robot Arm (SCARA) robot (DENSO HM-40A04). The 4DOF SCARA is the robot used for this PCB assembly project. This robot has a reach of 1,000 mm, speed of 8780 mm/s, Z-travel of 400 mm, maximum payload of 10kg, and 360-degree range of motion. The manufacturers listed repeatability for this robot is +-25 microns. The SCARA robot is mounted on a robot transfer unit (RTU) with a 2000 mm travel range. The system also features several modular, quick-change tools with discrete end-effectors, enabling automatic changing between tools for either of the industrial robots. The tools that were used for the PCB assembly include an electric gripper, pneumatic injection auger valve, and vacuum nozzle. Overall control of the NEXUS is accomplished via a NI PXI chassis running LabVIEW Real Time.

2.2 PCB Station

The PCB assembly station of the NeXus, shown in Figure 2, includes a PCB holder and separate component cut-tape holders. The system is mounted on a vibration control platform, an optical table. Its removable tool fixtures include 1.0 mm inner diameter vacuum nozzle (Juki 504) for picking up the components. A hollow shaft stepper motor rotates the nozzle 360 degrees with 800 steps per rotation providing a 0.45-degrees precision step size.

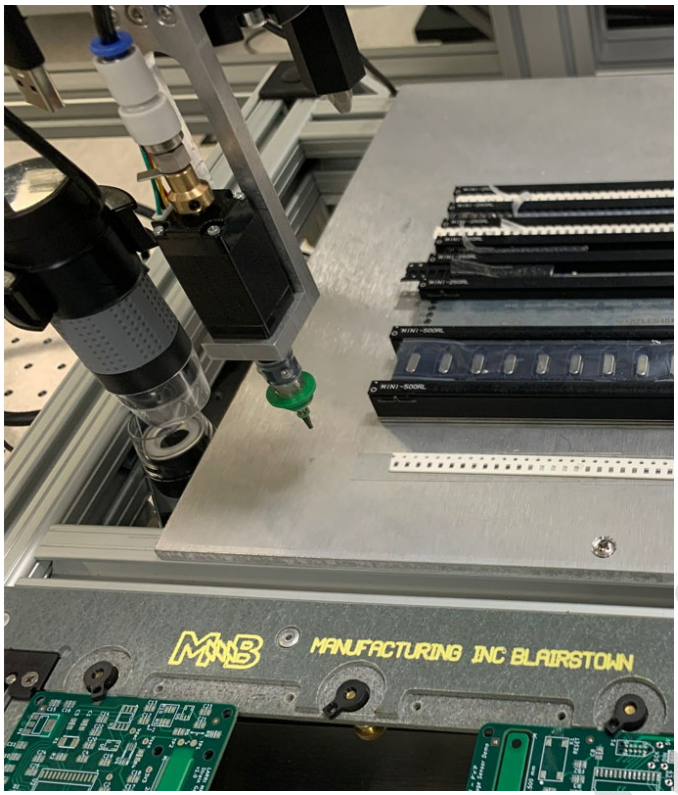

FIGURE 2: VACUUM NOZZLE PLACING COMPONENTS ON PCB IN THE NEXUS SYSTEM

For the experiments presented in this paper a surface mount capacitor, type X7R size 0805 was used. The size code 0805 refers to the length (0.08inch) and width (0.05inch). The manufacturer's listed dimensions and tolerances are listed in Table 1. A cut tape was used for the experiments that had a measured spacing between components of 4 mm.

TABLE 1: MANUFACTURES LISTED DIMENSIONS FOR SELECTED X7R CAPACITOR

	DIMENSION (mm)		
SIZE CODE	Length	Width	Thickness
0805	2.0 +- 0.2	1.25 +- 0.2	1.35+- 0.2

The PCB design is shown in Figure 3. It shows the design drawing and the part location script as generated by the design software. This script is used in the Labview program to direct the SCARA robot to the component location in PCB reference frame as part of the PCB assembly. The PCB origin shown in Figure 3 must be determined as part of the calibration process along with the component locations.

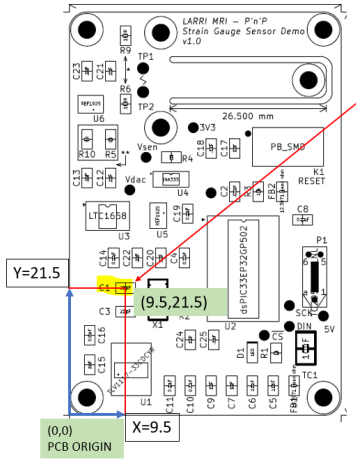

# R	Val	Package	PosX	PosY	Rot
C1	22pF	C0805	9.5	21.5	180
C2	.01uF	C0805	28	37.75	90
C3	22pF	C0805	9.5	17.5	180
C4	0.1uF	C0805	19.5	26.5	270
C5	10nF	C0805	34.5	5	90
C6	10uF	C0805	31	5	90

FIGURE 3: PCB BOARD DESIGN AND ASSEMBLY SCRIPT

2.3 Lean Robotic Micromanufacturing (LRM)

Lean Robotic Micromanufacturing is a design framework for multiscale (macro-micro) manufacturing work cells. LRM uses statistical analysis to assess and predict the success rate of a robot work cell, using the so-called High-yield Assembly Condition (HYAC) [10]. In this paper, we describe the LRM methodology for determining the minimum of control complexity necessary to reach reliable results for the PCB assembly with the large payload SCARA robot of the NeXus. Figure 4 provides a flow diagram of the LRM framework.

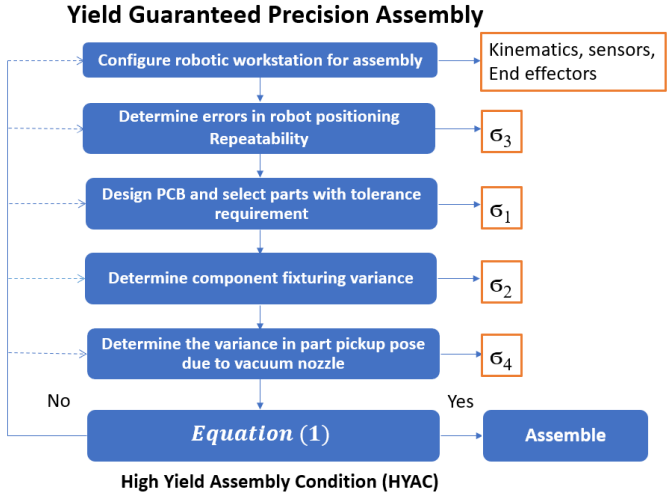

FIGURE 4: LEAN ROBOTIC MICROMANUFACTURING FLOW DIAGRAM

The first step is to configure the robotic workstation for assembly, which has been described in the previous sections. Step 2 of the framework is to determine the errors in the robot positioning by determining the robot's repeatability. In Step 3, we use the information from Step 2 to select or measure the maximum assembly tolerance of components. In the case of our PCB experiment, this step led to the selection of the component size and the oversizing of the PCB pads, shown in Figure 6.

These decisions provide a bound on the maximum assembly error tolerance. In Steps 4 and 5 we determine the variance in part location due to fixturing errors, and the variance in part pickup position due to prehension of the parts with the vacuum nozzle.

A statistical analysis was conducted to determine the necessary variances. We assumed a Gaussian distribution to represent the uncertainties in the robot work-cell, shown in Figure 4 and designed as σ_2, σ_3, and σ_4. These represent the standard deviation from either repeated experimental testing, or rational from precision measurements. Variances such as thermal expansion and surface tension were not included in the experiments as these would have effects negligible at the micron measurement scale. We also assume that the Gaussian distributions from the multiple sources are independent. Therefore, for independent Gaussian distributions, their variances can be added and the "central limit theorem" holds true [11].

$$\sigma_1^2 > \sigma_2^2 + \sigma_3^2 + \sigma_4^2 \qquad (1)$$

The inequality in equation (1) is the essence of what has been described as a high yield assembly condition (HYAC). It states that a 99.7% (3σ) assembly yield can be guaranteed if the combined uncertainty of locating the SMD components and positioning on the PCB is smaller than the assembly tolerance σ_1. The goal is to satisfy the HYAC by measuring the variances against the variance tolerance budget.

If HYAC is not met, assembly should not continue and variances must be reduced by various means such as design change, robot reconfiguration, offline planning, and/or online control schemes [9]. A σ_3 variance that satisfies the HYAC is chosen from an appropriate control mode for the P&P task, including open loop, closed loop, and calibrated operation defined below:

1. Open-loop control: relies on an assembly "script" and taught positions for the components and the X and Y Cartesian coordinates on the PCB.
2. Feed-forward control: control uses PCB layout information and calibration of the pickup robot.
3. Closed-loop control: control using active sensing based on servoing, for example using feedback from a camera.

Adding visual calibration and servoing controls is a common solution to increase the placement precision at the microscale. Although open-loop control is faster and requires less hardware resources than closed-loop control, it is also less accurate. With a workable solution, the HYAC can then serve as a discrete supervisory controller, applying various combinations of open-loop, closed-loop, and calibrated control modes throughout the process chain. A supervisory controller was not implemented in this paper because only one control method was determined to be necessary.

3. DESCRIPTION OF EXPERIMENTAL PROCEDURES

3.1 Errors in Robot Positioning

To determine the robot arm and tool changer variance σ_3, position measurements were taken on the X and Y coordinates with two Keyence LK-H008 displacement sensors with a listed repeatability of 5nm. The measurement sample rate was set to 10us (100kHz) for 500,000 samples. The target was a grey plastic box weighing 35g, shown in Figure 5. Deformation of the target was not a concern because the box was rigid, lightweight, and not subject to any external loads.

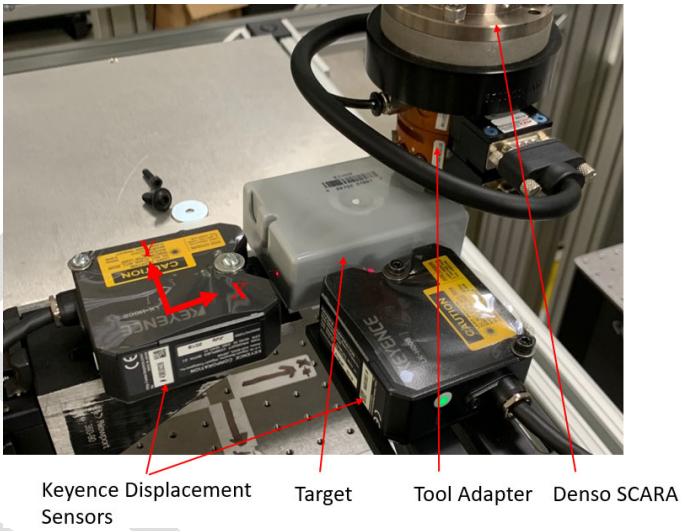

FIGURE 5 DISPLACEMENT SENSOR USED IN THE REPEATABILITY MEASUREMENT TEST

The SCARA robot followed the steps listed below to obtain repeatability data.

1. Move from an initial position to above the tool changer with the target.
2. Lower into position in the tool changer, activated the pneumatic lock to attach the tool and move up out of the tool changer.
3. Move target into view of the Keyence sensors, by giving the robot X, Y command positions X_c, Y_c.
4. Wait five seconds to allow system vibrations to dissipate.
5. Record attained positions X_{ai}, Y_{ai}.
6. Move back to the tool changer and return the tool adapter and target to the holder.
7. Return to the initial position.
8. Steps 1 through 7 were repeated 30 times to collect statistically significant data.

ISO 9283 Position Repeatability metrics [3] define our precision variance σ_3 according to the equations below. First, we define the mean of *N* planar positional measurements of the robot end-effector as:

$$\overline{X} = \frac{1}{N}\sum_{i=1}^{N} X_{ai} \qquad (2)$$

$$\overline{Y} = \frac{1}{N}\sum_{i=1}^{N} Y_{ai} \qquad (3)$$

In which l_i is the Cartesian coordinate vector variance from the separately measured X and Y variances. And $\bar{l}$ is the arithmetic mean of the vector variance from the 30 trials.

$$l_i = \sqrt{\left(X_i - \overline{X}\right)^2 + (Y_i - \overline{Y})^2} \quad (4)$$

$$\bar{l} = \frac{1}{N}\sum_{i=1}^{N} l_i \quad (5)$$

$$S_l = \sqrt{\sum_{i=1}^{N}(l_i - \bar{l})^2 \Big/ N - 1} \quad (6)$$

3.2 Tolerance Budget (σ_1)

The PCB pads were designed larger than necessary to provide a larger margin for variance. The PCB pads, as shown in Figure 6, measure 2.0 mm x 1.0 mm, whereas the component connection pad is only 1.25 mm x 0.4 mm. To maintain 100% of the component pad over the PCB pad would be ideal. However, given that the solder paste on the PCB will provide a measure of self-alignment, some measure less than 100% contact should provide proper contact. Assuming that the reflow of the solder paste for this size component will provide 75 – 150 microns of self-alignment [12]. Figure 6 shows the component offset 0.2 mm leaving 75% of the component pad on the PCB pad with 25% off. If the solder paste provides 0.1 mm of self-alignment, then this would bring the component pad into 100% contact with the PCB pad. Also, the solder paste filet profile can be expected to provide further contact if any gap remains [13] [12]. The factors affecting solder paste self-alignment depend on physical and thermal factors during reflow operations, however, in [14] C0603 solder paste self-alignment was found to average 249 microns. Therefore, using 200 microns as the three-sigma tolerance budget, one sigma equals 66.67 microns.

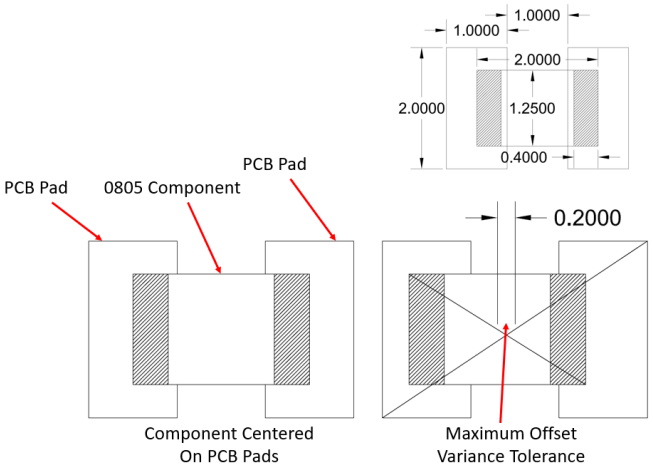

FIGURE 6: PART LOCATION TOLERANCE ON PCB PAD

3.3 Part Fixturing Variance (σ_2)

The cut tape used for this experiment has a predictable component spacing of 4 mm. Therefore, by teaching the robot the first component location and orientation, the following component locations are known. The cut-tape part holder uses embossed plastic cavities to hold the SMD parts. The cavity is larger than the part to allow it to be easily removed. With this larger cavity, the smaller part will have some variance relative to its position in the holder. The offset between the component's center and the cavity center would represent this variance. The gap clearance around all sides of the component was measured to be about 100 microns. This would allow a maximum diagonal displacement of 141.4 microns. Using 141.4 microns as our maximum three-sigma variance, one sigma equals 47.13 microns, see Figure 7.

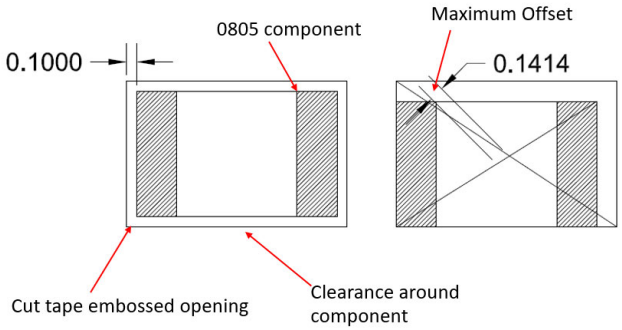

FIGURE 7: MAXIMUM PART FIXTURING VARIANCE

3.4 Vacuum Nozzle Pickup Variance (σ_4)

The part is picked up by positioning the vacuum nozzle at the center of the embossed opening, holding the component in the cut-tape. Vacuum is turned on to attach the part to the end of the nozzle. The robot moves the part to the PCB location; lowers the part, pressing the component onto the PCB pads with the nozzle spring tension; turns off the nozzle vacuum pressure; and raises up releasing the component. During the process of attaching and detaching the component from the nozzle, some movement and uncertainty of final position can occur. This variance is represented by σ_4. The experiment to test for this variance consists of a "dry placement" of a component without the presence of solder paste. This should represent a worst-case scenario since solder paste would reduce the amount of movement since the solder paste is sticky and would hold the part more stationary as it is released.

The experiment to test variance was as follows.

1. Place a component on the PCB pads.
2. Move robot over the component and pick it up.
3. Move robot to place the component over the up-facing camera.
4. Measure the position and orientation.
5. Place the component back to the same position and release.
6. Move robot up in the Z direction.
7. Steps 2 through 6 were repeated 30 times.

Since the nozzle errors will accumulate each iteration of the experiment, the error calculated will be the difference of measured values between each iteration.

3.5 Component Placement Experiment

A final component placement experiment was conducted to measure the repeatability of the robot arm placing SMD components on the PCB. This experiment reflects the combined errors from the three variances described in Figure 4, robot positioning (σ_3), fixturing (σ_2), and vacuum nozzle (σ_4). This experiment in intended to verify the HYAC condition in equation (1). If component placement in open-loop or calibrated operation is less than the design tolerance budget, then the operational high yield can be guaranteed, and no additional steps are needed such as redesign or adding visual servoing.

Steps for component placement experiment included:

1. Teach the robot the first component holder location.
2. Teach the robot the PCB origin (0,0) position.
3. Load the component PCB X, Y, and theta positions in a text file script derived from the PCB design files.
4. Move to the first component holder location and pick it up.
5. Move to scripted PCB location and orientation and place it down.
6. Move camera over component and measure actual X, Y, and theta.
7. Calculate error and record values.
8. Move to previous component location plus 4 mm in the X direction and pick it up.
9. Repeat steps 5 through 8 until reaching the end of the assembly script.

4. RESULTS AND DISCUSSION

4.1 Robot Positioning Error (σ_3)

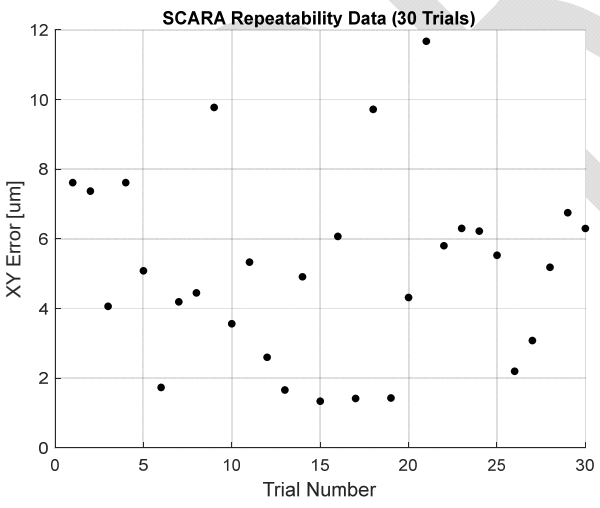

FIGURE 8: REPEATABILITY OF ROBOT END EFFECTOR (μm)

Figure 8 shows graphically the results of the robot end effector repeatability test. To determine the variance in robot position (σ_3), equations (2) through (6) were used. Equation (6) is the calculation for standard deviation needed for the HYAC analysis. These formulas correspond with ISO 9283 formulas as well. The standard deviation was calculated to be 13.0 microns. Therefore, σ_3 = 13.0 microns. This result makes sense given that the manufacturer's listed repeatability is 25 micron which would cover much heavier loads.

4.2 Vacuum Nozzle Pickup Variance (σ_4)

The vacuum nozzle pickup variance experiment results are shown in Figure 9. Because the experiment uses the robot arm to pick up and place the components, these errors would also reflect the robot error as well as the nozzle pickup error. The standard deviation found was 23.49 um.

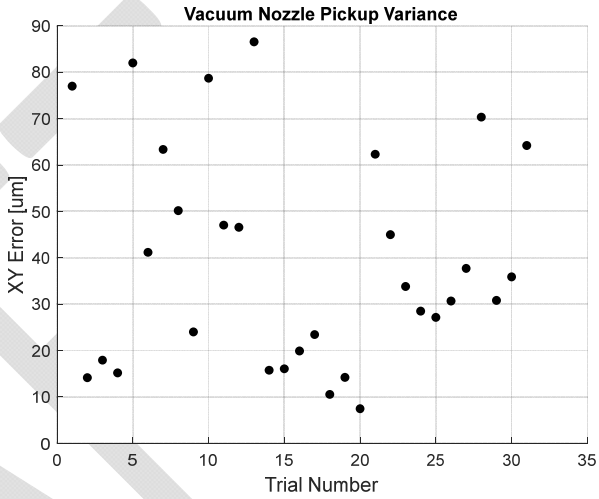

FIGURE 9: PART PICKUP NOZZLE ERROR RESULTS XY

4.3 Component Placement Experiment

As a type of verification of equation (1), the component placement test should reveal the combined errors of σ_2, σ_3, and σ_4. In order to obtain at least 30 trials of placing components on the PCB, six components were placed into separate locations on the PCB board giving 36 total data points. These results are shown in Table 2. Errors could have been reduced with further calibrations of the PCB origin and the component locations. For example, component C6 was measured consistently about 200 microns off of intended position. Nevertheless, these results are close to the measured cumulative errors found for σ_2, σ_3, and σ_4.

TABLE 2: COMPONENT PLACEMENT ERROR RESULTS

Trial #	Mean Placement Error of 6 Components (um)
1	168.7
2	150.9
3	168.9
4	130.3
5	160.5
6	121.4
Overall Mean	**150.1**
Overall Std Dev	**57.25**

4.4 Additional System Vibration Measurement

In addition to the repeatability, the Keyence sensors were used to test the steady state vibration on the optical table where the displacement sensors were mounted and to obtain a dynamic response capturing vibration damping from the robot and the support structure.

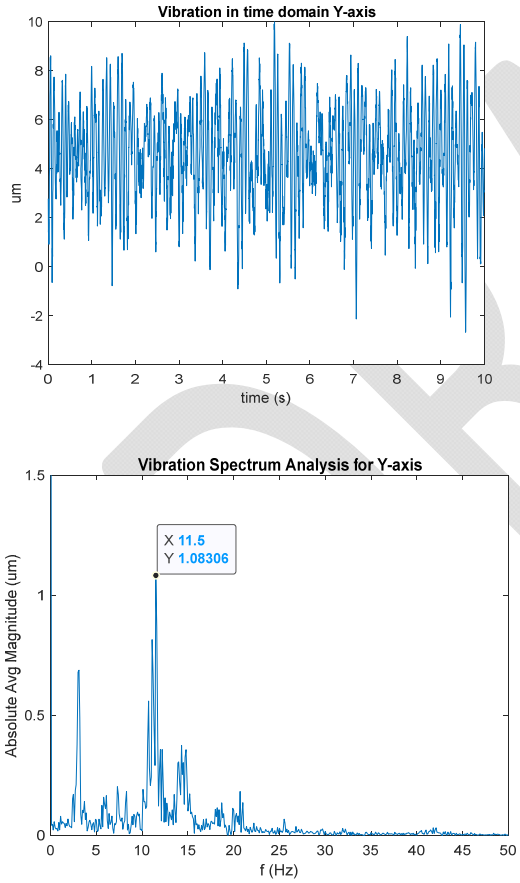

FIGURE 10: STATIONARY READING OF SCARA ARM HOLDING PLASTIC TARGET

The data shown in Figure 11 was collected by recording X and Y position of the target immediately after it entered the sensor area to capture settling time of the system. The settling time is estimated as 1.2 seconds. This information was useful in determining the delay time required to allow the system vibrations to dissipate to record static readings shown in Figure 11.

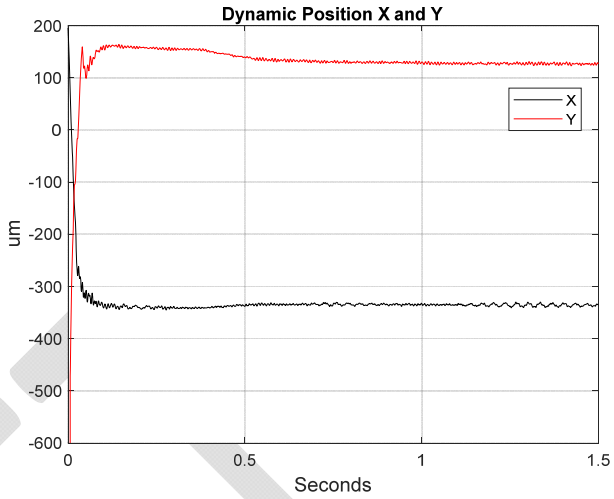

FIGURE 11: DYNAMIC XY POSITION SETTLE TIME

TABLE 3: RESULTS SHOWN IN REFERENCE TO EQUATION (1)

	Design Budget	Fixturing	Robot	Nozzle	
	σ_1	σ_2	σ_3	σ_4	Total
Std Dev	66.7	47.1	13.0	23.5	
σ^2	4444.4	2221.2	169.0	551.8	2942.0

5.CONCLUSIONS AND FUTURE WORK

In this paper, we experimentally evaluated the repeatability of a large 10 kg SCARA robot placing components on a printed circuit board. The Lean Robot Micromanufacturing (LRM) framework was implemented for the evaluation of the yield of the surface mount component pick and place operations. The LRM revealed the design tolerances and determined the system component errors, and control method to ensuring a high yield for PCB assembly.

The precision analysis results both met the High Yield Assembly Criteria (HYAC) of the LRM and was validated by experimental results. The SMD component placement experiment showed an average error within design tolerance of 200 µm. As a result, the control method needed to perform this task was “calibrated open-loop,” such that no visual servoing was required.

Future work will include the implementation of an up facing camera to provide correction for the fixturing error. Also, the control decision matrix for robot operation as described will be added, as well as process control development for automated solder dispensing and reflow.

ACKNOWLEDGEMENTS

This work was supported by National Science Foundation projects 1828355 and 1849213.

REFERENCES

[1] J. I. Ngadimin, F. I. Hariadi and M. I. Arsyad, "Design and Implementation of 3D Motion Control of Small Scale Pick and Place Surface-mount Technology Machine," in *2017 International Symposium on Electronics and Smart Devices*, 2017.

[2] A. Mousavi, A. Akbarzadeh, M. Shariatee and S. Alimardani, "Repeatability Analysis of a SCARA Robot with," in *RSI International Conference on Robotics and Mechatronics*, Tehran, 2015.

[3] ISO, "Manipulating Industrial Robots-Performance Criteria and Related Test Methods," International Organization for Standardization, 1998.

[4] J. F. Brethé, E. D. Vasselin, D. Lefebvre and B. Dakyo, "Determination of the repeatability of a kuka robot using the stochastic ellipsoid approach," in *Proceedings of the 2005 IEEE International Conference on Robotics and Automation*, 2005.

[5] K.-T. Park, C.-H. Park and Y.-J. Shin, "Performance Evaluation of Industrial Dual-Arm Robot," in *International Conference on Smart Manufacturing Application*, Gyeonggi-do,, 2008.

[6] D. O. Popa, R. Murthy and A. N. Das, "M3-Deterministic, Multiscale, Multirobot Platform," *IEEE TRANSACTIONS ON AUTOMATION SCIENCE AND ENGINEERING,* vol. 6, no. 2, 2009.

[7] J. Hsiao and K. Shivam, "Positioning Accuracy Improvement of Industrial," in *IEEE Acess*, 2020.

[8] C. Landgraf and K. Ernst, "A Hybrid Neural Network Approach for Increasing the Absolute," in *International Conference on Automation Science and Engineering*, Lyon, 2021.

[9] A. Das, "Automated 3D Microassembly with Precision Adjusted Hybrid Supervisory Controller," The University of Texas at Arlington, Arlington, 2009.

[10] A. Das, P. Zhang, W. Lee, D. Popa and H. Stephanou, "u3: Multiscale, Deterministic Micro-Nano Assembly System for Construction of On-Wafer Microrobots," in *IEEE International Conference on Robotics and Automation*, Roma, 2007.

[11] H. Tijms, Understanding Probability, Cambridge University Press, 2008.

[12] K. Dušek, M. Novák and A. Rudajevová, "Study of the Components Self–Alignment in Surface Mount Technology," in *35th Int. Spring Seminar on Electronics Technology*, 2012.

[13] K. Pan, J. H. Ha, H. Wang and J. X. Park, "An Analysis of Solder Joint Formation and Self-Alignment of Chip Capacitors," *IEEE TRANSACTIONS ON COMPONENTS, PACKAGING AND MANUFACTURING TECHNOLOGY,* vol. 11, no. 1, 2021.

[14] O. Krammer, Z. Radvanszki and Z. Illyefalvi-Vitez, "Investigating the Movement of Chip Components during Reflow Soldering," in *2nd Electronics Systemintegration Technology Conference*, Greenwich, 2008.

[15] D. Wei, A. Sherehiy, A. Tofangchi and D. O. Popa, "Precision Evaluation of NEXUS, a Custom Multi-Robot System for Microsystem Integration," in *Proceedings of the ASME 2021 16th International Manufacturing Science and Engineering Conference*, 2021.